HHS Public Access

Author manuscript

J Endocrinol. Author manuscript; available in PMC 2023 September 01.

Published in final edited form as:

J Endocrinol. 2023 September 01; 258(3): . doi:10.1530/JOE-23-0119.

BRD7 improves glucose homeostasis independent of IRS proteins.

Yoo Kim[1,2,3,*], **Junsik M. Lee**[1,*], **Youngah Han**[1], **Rongya Tao**[1,2], **Morris F. White**[1,2], **Renyan Liu**[1,2], **Sang Won Park**[1,2,#]

[1]Division of Pediatrics, Boston Children's Hospital, Boston, MA 02115, USA.

[2]Department of Medicine, Harvard Medical School, Boston, MA 02115, USA.

[3]Department of Nutritional Sciences, Oklahoma State University, Stillwater, OK 74078, USA.

Abstract

Bromodomain-containing protein 7 (BRD7) has emerged as a player in the regulation of glucose homeostasis. Hepatic BRD7 levels are decreased in obese mice, and the reinstatement of hepatic BRD7 in obese mice has been shown to establish euglycemia and improve glucose homeostasis. Of note, the upregulation of hepatic BRD7 levels activates the AKT cascade in response to insulin without enhancing the sensitivity of the insulin receptor (InsR)-insulin receptor substrate (IRS) axis. In this report, we provide evidence for the existence of an alternative insulin signaling pathway that operates independently of IRS proteins, and demonstrate the involvement of BRD7 in this pathway. To investigate the involvement of BRD7 as a downstream component of the InsR, we utilized liver-specific InsR knockout mice. Additionally, we employed liver-specific IRS1/2 knockout mice to examine the requirement of IRS1/2 for the action of BRD7. Our investigation of glucose metabolism parameters and insulin signaling unveiled the significance of InsR activation in mediating BRD7's effect on glucose homeostasis in the liver. Moreover, we identified an interaction between BRD7 and InsR. Notably, our findings indicate that the presence of IRS1/2 is not necessary for BRD7's regulation of glucose metabolism, particularly in the context of obesity. The upregulation of hepatic BRD7 exerts a significant effect on reducing blood glucose levels and restoring glucose homeostasis in high-fat diet-challenged liver-specific IRS1/2 knockout mice. These findings highlight the presence of an alternative insulin signaling pathway that operates independently of IRS1/2 and offer novel insights into the mechanisms of previously unknown insulin signaling in obesity.

[#]Corresponding author - Sang Won Park (sangwon.park@childrens.harvard.edu).
[*]Co-First authors.

Declaration of Interests

The authors declare that they have no competing interests that could be perceived as prejudicing the impartiality of the research reported.

Contribution statement

SWP formulated the hypothesis, and both SWP and YK designed the studies. YK, JL, YH, RT, RL, and SWP performed the experiments. YK, JL, and SWP analyzed the data. SWP and MFW provided critical research guidance. YK and JL prepared the figures. JL, YK, and SWP wrote the manuscript.

Keywords

BRD7; Insulin receptor signaling; Glucose metabolism; Insulin receptor substrates

Introduction

Type 2 diabetes is characterized by the progressive development of hyperglycemia and insulin resistance, which can lead to the development of various health complications, including cardiovascular disease, renal failure, retinopathy, and impaired limb function. In the past four decades, the prevalence of adults with type 2 diabetes has nearly quadrupled (Zheng et al., 2018), mirroring the escalating rates of obesity, a known risk factor for the development of type 2 diabetes. However, the precise underlying link between obesity and the pathogenesis of type 2 diabetes remains incompletely understood. It is crucial to unravel the mechanisms responsible for elevated blood glucose levels and insulin resistance in the context of obesity to effectively address the challenge of type 2 diabetes.

Insulin exerts its actions primarily through the insulin receptor (InsR), which functions as a transmembrane tyrosine kinase. Upon activation, the InsR undergoes a conformational change, leading to autophosphorylation, recruitment of substrates, and initiation of various cellular responses, including glucose transport, protein and lipid synthesis, and cell differentiation (Boucher et al., 2014). In the liver, insulin stimulation plays a crucial role in suppressing gluconeogenesis, promoting glycogenesis, and enhancing triglyceride synthesis (Haeusler et al., 2018, Rui, 2014).

Liver-specific insulin receptor knockout (LIRKO) mice, which lack InsR specifically in the liver, exhibit mild fasting hyperglycemia (Michael et al., 2000, Titchenell et al., 2015) and elevated insulin levels (Michael et al., 2000, Titchenell et al., 2015, InSug et al., 2015). Furthermore, they display reduced serum triglycerides and increased susceptibility to atherosclerosis (Michael et al., 2000, Biddinger et al., 2008). As the loss of hepatic InsR compromises the suppression of gluconeogenesis, LIRKO mice progressively develop fasting hypoglycemia and display liver failure (Michael et al., 2000).

IRS proteins play a critical role as adaptor molecules that bind to InsR in response to insulin stimulation. The functions of IRS proteins have been elucidated through studies utilizing genetic knockout models. Liver-specific IRS1 and IRS2 double KO (IRS DKO) mice display impaired glucose tolerance and insulin resistance (Kubota et al., 2008, Dong et al., 2008). IRS DKO mice exhibit an increased hepatic glucose production rate accompanied by elevated expression levels of glucose 6-phosphatase and phosphoenolpyruvate carboxykinase (Kubota et al., 2008, Dong et al., 2008, Kubota et al., 2016). A study investigating the impact of nutrient stress on glucose homeostasis in the absence of IRS1/2 demonstrated that high-fat diet (HFD)-fed IRS DKO mice display hyperglycemia, glucose intolerance, and insulin resistance (Guo et al., 2009). Additionally, HFD-fed IRS DKO mice exhibit elevated fasting insulin levels and reduced triglyceride concentrations in both plasma and the liver (Guo et al., 2009).

Following insulin-induced activation of IRS, IRS recruits phosphatidylinositol 3-kinase (PI3K), which comprises the regulatory subunit p85 and the catalytic subunit p110. The binding of p85 to IRS relieves its inhibition of the catalytic p110 subunit activity, leading to the subsequent activation of protein kinase B (AKT). The p85 subunit exists in two isoforms, p85α and p85β, which can exist as monomers (Ueki et al., 2002), homodimers (Luo et al., 2005), or heterodimers that are dissociated upon insulin stimulation (Park et al., 2010). Notably, p85 monomers interact with the spliced form of X-box binding protein 1 (XBP1s), a transcription factor that plays a critical role in maintaining endoplasmic reticulum (ER) homeostasis (Park et al., 2014). This interaction is essential for XBP1s nuclear translocation, which alleviates ER stress.

Bromodomain-containing protein 7 (BRD7) belongs to the family of bromodomain-containing proteins (Sanchez and Zhou, 2009). Complete deletion of both BRD7 alleles in mice leads to embryonic lethality (Kim et al., 2016). Heterozygous BRD7 knockout mice and liver-specific BRD7 knockout mice exhibit significant weight gain when fed on a HFD (Lee et al., 2019, Park and Lee, 2020). Conversely, a significant decrease in BRD7 levels is observed in the liver of HFD-induced obese mice and genetically obese *ob*/*ob* mice (Park et al., 2014). Restoring BRD7 levels in the liver of obese and type 2 diabetic mice results in the re-establishment of euglycemia and the restoration of glucose homeostasis (Park et al., 2014). BRD7 enhances insulin signaling by promoting AKT phosphorylation upon insulin stimulation in the liver of obese mice (Park et al., 2014, Lee et al., 2021). These findings strongly suggest that BRD7 is involved in the regulation of glucose metabolism and functions as a component of the insulin signaling pathway. Of interest, it has been shown that the upregulation of hepatic BRD7 levels activates the IRS1PI3KAKT cascade in response to insulin stimulation, without increasing the sensitivity of the InsRIRS1 axis (Park et al., 2014). However, the precise underlying mechanisms of this observation remain incompletely understood. In this report, we provide evidence demonstrating that BRD7 participates in an alternative insulin signaling pathway that operates independently of IRS1/2.

Material and methods

Immunoprecipitation

For immunoprecipitation experiments, cell or tissue lysates were incubated with the appropriate antibody on a rotator for 2–4 hours at 4°C. Subsequently, 15–20 μL of protein G Sepharose or mixed protein A/G magnetic beads were added to the lysates and incubated on a rotator for an additional 1 hour at 4°C. The beads were then washed three times with lysis buffer and collected either by centrifugation or using magnets. To elute the bound proteins, 25–30 μL of 2× Laemmli buffer was added to the beads, and the mixture was boiled at 100°C for 5 minutes. The eluted proteins were resolved on SDS-PAGE and further analyzed as described in the western blotting section. In pulldown experiments, cell lysates were incubated with S-protein agarose beads for 4 hours at 4°C. The resulting protein complexes were analyzed by western blotting, and all the blots were quantified using ImageJ.

Adenovirus (Ad) production and infection

The BRD7 cDNA (NCBI reference sequence ID: NM_012047.2) was introduced into a serotype 5 adenoviral vector known for its specific targeting of liver cells, as previously described (Park et al., 2014, Golick et al., 2018). Subsequently, the adenoviral vectors were transfected into 293A cells. The culture media was replaced with fresh media every 3 days. When the cytopathic effect reached 80% of the cells, cells and media were collected and transferred to 15 mL conical tubes. The cells were lysed by three cycles of freezing in liquid nitrogen and thawing at 37°C followed by centrifugation at 1,200 × g for 30 minutes at room temperature. The supernatant containing the adenovirus particles was collected and stored at −80°C. To generate subsequent generations of adenovirus, 293A cells were infected with the adenovirus and cultured in DMEM with 5% FBS, 100 U/mL penicillin, and 100 μg/mL streptomycin. Upon reaching 80% cytopathic effect, the cells were pelleted by centrifugation at 1,200 × g for 20 minutes at room temperature, resuspended in DMEM with 1% FBS, and lysed to harvest the virus as described above. For *in vitro* experiments using adenovirus, the adenovirus was added to the media and incubated for 16 hours. For *in vivo* experiments using adenovirus, Ad-BRD7 and Ad-LacZ (Vector Biolabs, 1080-HT) were purified using a cesium chloride density gradient by Vector Biolabs (Malvern, PA, USA).

Mouse lines and husbandry

All animal experiments were conducted in accordance with the policies and guidelines set by the AAALAC (Association for Assessment and Accreditation of Laboratory Animal Care International) and under the supervision of veterinarians at Animal Resources Boston Children's Hospital (ARCH). The experimental protocols were approved by the Institutional Animal Care and Use Committee of Boston Children's Hospital. The liver-specific insulin receptor knockout (LIRKO) mice used in this study were provided by Dr. Sudha Biddinger at Boston Children's Hospital (Boston, MA, USA). The liver-specific bromodomain-containing protein 7 knockout mice (LBKO) were generated by our group as described previously (Golick et al., 2018). All animals were housed in a specific-pathogen-free facility at Boston Children's Hospital, where temperature and humidity were controlled. The mice were kept on a 12-hour light (7:00 a.m.–7:00 p.m.) and dark (7:00 p.m.–7:00 a.m.) cycle. All experiments were performed during the light cycle. Mice were randomly assigned to feed either a normal chow diet (NCD, 14% calories from fat, LabDiet 5P76, St. Louis, MO, USA) or an irradiated high-fat diet (HFD, 45% calories from fat, Research Diets Inc. D12451i, New Brunswick, NJ, USA).

Adenovirus tail vein injection

Adenovirus stocks were diluted with saline to a final volume of 100 μL per mouse. Mice were restrained using a restrainer, and their tails were mildly heated with a heating lamp to promote vasodilation. Using a 30-gauge needle, the adenovirus was injected through the tail vein. To prevent the backflow of the viral solution, mild pressure was applied at the injection site immediately after the injection.

Glucose tolerance test (GTT), insulin tolerance test (ITT), and pyruvate tolerance test (PTT)

To perform a GTT, mice were fasted for 15 hours (6:00 p.m. – 9:00 a.m.). Fasted blood glucose levels were measured using blood from the tail vein. D-glucose was diluted in saline to a volume of 100–150 μL and injected intraperitoneally at the following dosages: 1.2 g/kg for HFD-fed LIRKO mice; 1.5 g/kg for HFD-fed LIRKO control mice; and 1.0 g/kg for HFD-fed IRS DKO mice. Blood glucose levels were measured prior to the intraperitoneal injection, and at 15, 30, 60, 90, and 120 minutes post-injection. For IRS DKO mice, blood glucose was also measured at 150 minutes post-injection. To perform an ITT, mice were fasted for 6 hours (8:00 a.m.–2:00 p.m.). Insulin was diluted in saline to a volume of 100 μL and injected intraperitoneally. The doses used were 2.0 IU/kg for HFD-fed LIRKO mice; 1.0 IU/kg for HFD-fed LIRKO control mice; and 2.0 IU/kg for HFD-fed IRS DKO mice and their control mice. For a PTT, mice were fasted for 14 hours (7:00 p.m.–9:00 a.m.). Sodium pyruvate was dissolved in saline and the pH of the solution was adjusted to 7.4 with sodium hydroxide. The pH-adjusted solution was diluted in saline to a volume of 200–400 μL and injected intraperitoneally at a dose of 2.0 g/kg. Blood glucose levels were measured as described above for the GTT.

Statistics

Body weight levels, GTT, ITT, and PTT were analyzed using a two-way ANOVA repeated measure mixed ANOVA. Quantitative data, such as AUC, western blot band density, and qPCR results, were analyzed using an unpaired Students' t-test after the outlier test. The significance levels were set at $\alpha=0.05$. The mean values are reported as the mean ± SEM. Statistical analysis was conducted using GraphPad Prism software (Prism 9; GraphPad Inc., San Diego, CA, USA). The level of significance was indicated by asterisks: *$p\leq0.05$, **$p\leq0.01$, and ***$p\leq0.001$, which were considered statistically significant.

Results

BRD7 does not establish euglycemia in obesity in the absence of insulin receptor

In our previous study, we demonstrated that the upregulation of BRD7 improves glucose homeostasis in obese mice (Park et al., 2014). In this study, we sought to investigate if the presence of the InsR is necessary for BRD7's effect on glucose metabolism regulation and whether BRD7 acts as a downstream protein of InsR. To address these questions, we aimed to examine the impact of hepatic BRD7 overexpression in mice with a liver-specific InsR knockout during a high-fat diet (HFD) challenge comprising 45% of total calories from fat. To verify the effectiveness of the HFD on blood glucose levels, we first placed WT mice on either a normal chow diet (NCD) or a HFD for 8 weeks. The measurement of blood glucose levels revealed a significant increase in both the 6-hour fasted and fed states for the HFD-fed mice (Supplementary Fig. 1A and 1B). We then subjected 4-week-old LIRKO and control mice to a HFD for 7.5 weeks. Subsequently, the mice were injected with Ad-BRD7 or Ad-LacZ (control) through the tail vein at a dose of 5×10^7 plaque forming units (pfu)/g. On day 8 post-injection, no significant difference in body weights was observed between the mice injected with Ad-LacZ and Ad-BRD7 in both the LIRKO and control groups (Fig. 1A). The blood glucose levels measured in the fed state indicated a significant decrease in control mice injected with Ad-BRD7 compared to those injected with Ad-LacZ (Fig. 1B,

left). However, there was no difference in fed blood glucose levels between the Ad-BRD7- and Ad-LacZ-injected LIRKO mice (Fig. 1B, right). A similar pattern was observed when blood glucose was measured after 6 hours of fasting, in which Ad-BRD7 injection decreased blood glucose in control mice, but not in LIRKO (Fig. 1C). To investigate the potential impact of an extended HFD challenge, we replicated the experiment with LIRKO mice, subjecting them to an additional 3 weeks of HFD feeding. After 11 weeks of HFD challenge, mice were injected with Ad-BRD7 or Ad-LacZ with the same dose and method. The results showed no difference in body weights and blood glucose levels between Ad-BRD7- and Ad-LacZ-injected LIRKO mice at the 6-hour fasting state on day 8 post-injection (Fig. 1D). Our data demonstrate that InsR is required for BRD7 to reduce blood glucose levels in HFD-challenged obese mice.

To exclude any potential effects originating from other organs, we sought to assess the liver-targeting ability of adenovirus administered via the tail vein. To confirm the specific expression of Ad-BRD7 in the liver, we injected WT mice with Ad-BRD7 through the tail vein, and harvested various tissues, including the liver, pancreas, skeletal muscle, adipose tissue, lung, heart, and blood cells, on day 7 post-injection for analysis of BRD7 mRNA expression levels. The results showed that the adenovirus-mediated overexpression of BRD7 was significantly elevated exclusively in the liver, providing evidence that the observed effects on glucose homeostasis are specifically attributed to the effects of Ad-BRD7 in the liver and not due to extraneous BRD7 overexpression in other tissues (Supplementary Fig. 2).

The insulin receptor is required for BRD7 to establish glucose homeostasis

To assess the glucose disposal rate on HFD-fed LIRKO mice that were injected with Ad-BRD7 or Ad-LacZ (control) at a dose of 5×10^7 pfu/g via the tail vein, we conducted a glucose tolerance test (GTT) on day 8 post-injection. The results showed a significant improvement in the Ad-BRD7-injected control mice compared to the Ad-LacZ-injected control mice (Fig. 2A). However, this improvement was compromised in LIRKO mice lacking InsR (Fig. 2B), suggesting that InsR is necessary for BRD7 to improve glucose tolerance in obese mice. Furthermore, an insulin tolerance test (ITT) was performed on day 6 post-injection to evaluate insulin sensitivity. The results showed a significant decrease in area under the curve (AUC) in the Ad-BRD7-injected control mice compared to the Ad-LacZ-injected control mice (Fig. 2C). In contrast, there was no difference observed between Ad-BRD7- and Ad-LacZ-injected LIRKO mice (Fig. 2D). These findings indicate that BRD7's ability to enhance glucose homeostasis relies on the presence of InsR. Overexpression of BRD7 resulted in a significant increase in the phosphorylation levels of AKT at residues Thr308 and Ser473 in control mice at the 6-hour fasted state (Fig. 2E). However, this BRD7-mediated increase in AKT phosphorylation was not observed in the absence of InsR (Fig. 2F). These results further support the requirement of InsR for BRD7 to modulate glucose homeostasis.

Restoration of insulin receptor and upregulation of BRD7 in the liver reinstate glucose homeostasis in HFD-challenged LIRKO mice

To determine whether the impaired glucose homeostasis restoration achieved by overexpressing BRD7 in HFD-challenged LIRKO mice is solely attributed to the absence of InsR, we re-established InsR expression and overexpressed BRD7 in the liver of LIRKO mice by administering Ad-InsR and Ad-BRD7, respectively, at a dose of 4×10^7 pfu/g through the tail vein. Ad-LacZ was used as a control, ensuring equal viral load in each mouse. No significant difference in body weights was observed between the two groups (Fig. 3A). Blood glucose levels measured after a 6-hour fasting period displayed a significant reduction in the Ad-InsR/Ad-BRD7-injected group (Fig. 3B). A GTT performed on day 4 post-injection showed an improved glucose disposal rate in the Ad-InsR/Ad-BRD7-injected group (Fig. 3C). Furthermore, an ITT performed on day 6 post-injection revealed enhanced insulin sensitivity in the Ad-InsR/Ad-BRD7-injected group (Fig. 3D). Collectively, the restoration of InsR reversed the observed lack of effect of BRD7 in LIRKO mice, indicating the essential role of InsR in mediating the beneficial effects of BRD7 on improving glucose homeostasis.

BRD7 interacts with the insulin receptor

Considering the essential role of InsR in improving glucose homeostasis by BRD7, we asked if BRD7 interacts with InsR. For this purpose, we infected rat hepatoma Fao cells with Ad-BRD7 or Ad-LacZ (control), followed by immunoprecipitation using an InsR-specific antibody. Immunoblotting analysis showed the co-immunoprecipitation of BRD7 with InsR (Fig. 4A), indicating their interaction. To verify the specificity of the bands adjacent to the BRD7-specific bands in the immunoblot, we took measures to eliminate any non-specific interactions. We constructed a plasmid encoding S-tagged BRD7 (pSRα-HA-S-BRD7) and transfected HEK293 cells, while employing the backbone plasmid as a control. By utilizing S-protein agarose beads, we selectively captured the S-tagged BRD7 from cell lysates and subjected the precipitate to immunoblotting using an InsR-specific antibody. The results validated the specific interaction between BRD7 and InsR devoid of non-specific bands (Fig. 4B). To further demonstrate the specificity of this interaction between InsR and BRD7, we conducted additional experiments using different cell types and *in vivo* samples. Firstly, we repeated the co-immunoprecipitation experiment using immortalized mouse embryonic fibroblasts (MEFs) derived from WT or mice that lack InsR. The interaction between InsR and BRD7 was observed in WT MEFs, while no interaction was detected in InsR knockout MEFs, providing further evidence for the specificity of the observed bands (Fig. 4C). To investigate this interaction in hepatocytes, we isolated primary hepatocytes from 12-week-old C57Bl/6J male mice and infected them with Ad-BRD7 alone or in combination with Ad-InsR. Co-immunoprecipitation of BRD7 with endogenous InsR was observed in the primary hepatocytes, confirming the interaction in this cell type (Fig. 4D). Next, we collected the liver from WT and liver-specific BRD7 knockout (LBKO) mice, and performed the co-immunoprecipitation experiment. Immunoprecipitation of endogenous InsR from the total lysates, followed by immunoblotting with a BRD7-specific antibody, revealed co-immunoprecipitation of BRD7 with InsR in the liver of the WT mouse. However, no interaction was observed in the liver of the LBKO mouse, providing additional confirmation of the interaction between InsR and BRD7 (Fig. 4E).

To explore the dynamic nature of the InsR-BRD7 interaction under physiological conditions, we conducted an investigation to determine if this interaction is influenced by external nutrient availability. To achieve this, we administered Ad-BRD7 or Ad-LacZ (control) to C57Bl/6J mice through the tail vein at a dose of 5×10^7 pfu/g. On day 6 post-injection, the mice were subjected to a 24-hour fasting period and then sacrificed either in the fasted state or after 1 hour of *ad libitum* refeeding. Subsequently, we performed a co-immunoprecipitation experiment using total lysate from liver tissues. The interaction between InsR and BRD7 was found to be increased in mice after 1 hour of refeeding (Fig. 4F), indicating a responsive nature of this interaction to nutrient availability.

Taking into consideration the tyrosine kinase activity of InsR, we sought to investigate the potential phosphorylation of BRD7 on tyrosine residues. To explore this, we stimulated primary hepatocytes isolated from a C57Bl/6J mouse with insulin (100 nM) for 15 minutes. Subsequently, we performed immunoprecipitation of BRD7, followed by a western blot analysis for phospho-tyrosine (pY). The findings revealed an increase in phosphorylation of BRD7 on tyrosine residues (Fig. 4G). Furthermore, we isolated primary hepatocytes from 8-week-old male liver-specific BRD7 transgenic (LBTg) mice (Golick et al., 2018) and treated them with insulin (100 nM) for 0, 15, or 60 minutes. The western blot showed the phosphorylation of BRD7 on tyrosine residues following insulin stimulation (Fig. 4H). These findings illuminate the previously undiscovered interaction between InsR and BRD7, establishing BRD7 as an integral component of the InsR signaling pathway.

BRD7 improves glucose homeostasis in the absence of IRS1/2

IRS1/2 play crucial roles as key components in the insulin signaling pathway, serving as major mediators between InsR and downstream effector proteins. Therefore, we sought to investigate whether IRS1/2 is involved in mediating the effect of BRD7 on glucose homeostasis. Considering that BRD7 improves glucose homeostasis in obesity, we subjected 4-week-old IRS DKO mice to a HFD for 8–11 weeks and injected them with Ad-BRD7 or Ad-LacZ (control) through the tail vein at a dose of 1.5×10^8 pfu/g. There was no significant difference in body weights between the Ad-BRD7- and Ad-LacZ-injected groups on days 8–11 post-injection (Fig. 5A). However, blood glucose levels measured on days 8–10 post-injection showed a significant reduction in the Ad-BRD7-injected IRS DKO mice compared to the Ad-LacZ-injected group (Fig. 5B). Furthermore, a GTT performed on day 5 post-injection revealed significantly improved glucose disposal in Ad-BRD7-injected mice (Fig. 5C). The AUC calculated from an ITT performed on day 8 post-injection showed a reduction in Ad-BRD7-injected mice with a p-value of 0.065 (Fig. 5D). Although the p-value did not reach its significance, it is worth noting that IRS DKO mice inherently exhibit considerable individual variation in blood glucose levels (Kubota et al., 2008, Dong et al., 2008).

Next, considering the dysregulated hepatic gluconeogenesis in IRS DKO mice (Guo et al., 2009), we conducted a pyruvate tolerance test (PTT) on day 9 post-injection. The Ad-BRD7-injected group exhibited a significantly reduced gluconeogenic response to the pyruvate challenge (Fig. 5E). Furthermore, upregulation of BRD7 in IRS DKO mice resulted in significant increases in the phosphorylation levels of AKT at residues Thr308 and Ser473

in the 6-hour fasted state (Fig. 5F). In our previous study, we reported that BRD7 increases the phosphorylation of GSK3β at residue Ser9 (Golick et al., 2018). This increase in GSK3β phosphorylation was still observed even in the absence of IRS1/2 (Fig. 5F). These findings indicate that BRD7 plays a role in the insulin signaling pathway independent of the IRS-AKT axis.

Discussion

The role of IRS1/2 in the canonical insulin signaling pathway has been widely acknowledged and extensively studied. Previous studies have provided evidence that phosphorylation of AKT is not affected by insulin stimulation in the absence of IRS1/2 (Dong et al., 2006, Guo et al., 2009, Kubota et al., 2008). Meanwhile, recent findings have shed light on the presence of an alternative insulin signaling pathway that operates independently of the canonical InsRIRS1/2AKT insulin signaling pathway (Lu et al., 2012, Titchenell et al., 2015, Guo et al., 2009). For instance, the deletion of forkhead box protein O1 (FoxO1) in the liver in the absence of IRS1/2 reverses diabetic features observed in IRS1/2 DKO mice (Dong et al., 2008). Similarly, the deletion of FoxO1 in the liver in the absence of AKT restores insulin responsiveness and displays normal postprandial regulation (Lu et al., 2012). Notably, GSK3β phosphorylation is observed in response to insulin even in the absence of IRS proteins (Dong et al., 2008). In our previous study, we also demonstrated that BRD7 increases the phosphorylation of GSK3β even in the absence of AKT (Golick et al., 2018). These findings strongly suggest the existence of an insulin signaling pathway that functions independently of the canonical InsR-IRS1/2 axis exists.

In this work, we have demonstrated that the overexpression of BRD7 leads to increased phosphorylation of AKT and GSK3β and improved glucose homeostasis, even in the absence of IRS1/2. The observed reduction in glycemic excursion following pyruvate administration in IRS DKO mice injected with Ad-BRD7 suggests that BRD7 suppresses gluconeogenesis by BRD7 through a mechanism independent of the canonical IRS1/2-dependent insulin signaling pathway. These findings provide evidence for the existence of an alternative IRS1/2-independent insulin signaling pathway and highlight the involvement of BRD7 in regulating glucose homeostasis within this pathway (Fig. 6). We speculate that these pathways serve distinct purposes and are activated by specific cues, the nature of which is currently unknown. The precise mechanisms by which BRD7 functions in both the canonical and alternative signaling pathways to contribute to metabolic homeostasis require further investigation.

In this study, we specifically focused our research on the liver for several reasons. Firstly, the liver plays a central role in gluconeogenesis and is a key target organ for insulin action. It is involved in other processes, including the maintenance of stable blood glucose levels, such as glycogen synthesis and glucose uptake. Secondly, the liver has already been recognized as a significant site where BRD7 exerts influence (Park et al., 2010). While some aspects of BRD7's role in the liver have been elucidated, much remains unknown and requires further investigation. Thirdly, hepatic dysfunction is a common feature of obesity and type 2 diabetes, highlighting the relevance of investigating the role of BRD7 in the liver under these conditions. Therefore, we built upon our previous studies and provided further insight

into the mechanism of BRD7 in the liver, as well as its potential implications for maintaining metabolic homeostasis.

Meanwhile, BRD7 exhibits ubiquitous expression in various tissues and cells. Therefore, it is possible that BRD7 has a role in other metabolic tissues as well, particularly when considering the complex interplay of insulin signaling, which involves the collaborative contributions of multiple tissues (White and Kahn, 2021). Therefore, alterations in hepatic metabolism can have profound effects on insulin sensitivity in other organs. For instance, the absence of hepatic IRS1/2 leads to the development of insulin resistance in WAT and IRS DKO mice experience increased lipolysis due to impaired insulin sensitivity (Tao et al., 2018). Of interest, the inactivation of FoxO1 in the liver of IRS DKO restores insulin signaling in WAT (Tao et al., 2018). Therefore, it is plausible that the BRD7 upregulation in the liver of IRS DKO mice may also exert effects on organs beyond the liver, which warrants further investigation.

In summary, our work provides novel insights into the role of BRD7 as an interacting partner of InsR and its involvement in an IRS1/2-independent alternative insulin signaling pathway. By further exploring and characterizing this signaling pathway, we can gain a better understanding of the intricate balance between the canonical and non-canonical insulin signaling pathways. This knowledge holds promise in developing innovative therapeutic approaches to address metabolic disturbances and their associated complications, particularly in the context of obesity.

Supplementary Material

Refer to Web version on PubMed Central for supplementary material.

Acknowledgments

We thank Dr. Sudha Biddinger for generously providing the LIRKO mice, Dr. Ron Khan for supplying the InsR-expressing plasmid and Dr. Ying Huang for contributing the pSRα-HA-S backbone plasmid.

Funding

This work was supported by grants from the National Institute of Diabetes and Digestive and Kidney Diseases of the National Institute of Health (R01DK118244), the American Heart Association (18IPA34140057), and a startup fund from Boston Children’s Hospital provided to SWP; and a startup fund from Oklahoma State University provided to YK.

Abbreviations

AKT	protein kinase B
BRD7	bromodomain-containing protein 7
ER	endoplasmic reticulum
FBS	fetal bovine serum
GTT	glucose tolerance test
HFD	high-fat diet

HRP	horseradish peroxidase
InsR	insulin receptor
IRS	insulin receptor substrate
ITT	insulin tolerance test
LBKO	liver-specific bromodomain-containing protein 7 knockout mice
LIRKO	liver-specific insulin receptor knockout mice
IRS DKO	Liver-specific IRS1 and IRS2 double KO mice
PI3K	phosphatidylinositol 3-kinase
PTT	pyruvate tolerance test
PVDF	polyvinylidene fluoride
SEM	standard error of the mean
T2D	type 2 diabetes
TBS	Tris-buffered saline
TBS-T	TBS with 0.05% Tween20
WT	wild-type
XBP1	X-box binding protein 1

Reference

BIDDINGER SB, HERNANDEZ-ONO A, RASK-MADSEN C, HAAS JT, ALEMÁN JO, SUZUKI R, SCAPA EF, AGARWAL C, CAREY MC & STEPHANOPOULOS G. 2008. Hepatic insulin resistance is sufficient to produce dyslipidemia and susceptibility to atherosclerosis. Cell Metab, 7, 125–134. [PubMed: 18249172]

BOUCHER J, KLEINRIDDERS A. & KAHN CR 2014. Insulin receptor signaling in normal and insulin-resistant states. Cold Spring Harb Perspect Biol, 6, a009191.

DONG X, PARK S, LIN X, COPPS K, YI X. & WHITE MFJTJOCI 2006. Irs1 and Irs2 signaling is essential for hepatic glucose homeostasis and systemic growth. 116, 101–114.

DONG XC, COPPS KD, GUO S, LI Y, KOLLIPARA R, DEPINHO RA & WHITE MF 2008. Inactivation of hepatic Foxo1 by insulin signaling is required for adaptive nutrient homeostasis and endocrine growth regulation. Cell Metab, 8, 65–76. [PubMed: 18590693]

GOLICK L, HAN Y, KIM Y. & PARK SW 2018. BRD7 regulates the insulin-signaling pathway by increasing phosphorylation of GSK3beta. Cell Mol Life Sci, 75, 1857–1869. [PubMed: 29127434]

GUO S, COPPS KD, DONG X, PARK S, CHENG Z, POCAI A, ROSSETTI L, SAJAN M, FARESE RV & WHITE MF 2009. The Irs1 branch of the insulin signaling cascade plays a dominant role in hepatic nutrient homeostasis. Mol Cell Biol, 29, 5070–83. [PubMed: 19596788]

HAEUSLER RA, MCGRAW TE & ACCILI D. 2018. Biochemical and cellular properties of insulin receptor signalling. Nat Rev Mol Cell Biol, 19, 31–44. [PubMed: 28974775]

INSUG O, ZHANG W, WASSERMAN DH, LIEW CW, LIU J, PAIK J, DEPINHO RA, STOLZ DB, KAHN CR & SCHWARTZ MWJNC 2015. FoxO1 integrates direct and indirect effects of insulin on hepatic glucose production and glucose utilization. 6, 1–15.

KIM Y, ANDRES SALAZAR HERNANDEZ M, HERREMA H, DELIBASI T. & PARK SW 2016. The role of BRD7 in embryo development and glucose metabolism. J Cell Mol Med, 20, 1561–70. [PubMed: 27444544]

KUBOTA N, KUBOTA T, ITOH S, KUMAGAI H, KOZONO H, TAKAMOTO I, MINEYAMA T, OGATA H, TOKUYAMA K. & OHSUGI MJCM 2008. Dynamic functional relay between insulin receptor substrate 1 and 2 in hepatic insulin signaling during fasting and feeding. 8, 49–64.

KUBOTA N, KUBOTA T, KAJIWARA E, IWAMURA T, KUMAGAI H, WATANABE T, INOUE M, TAKAMOTO I, SASAKO T. & KUMAGAI KJNC 2016. Differential hepatic distribution of insulin receptor substrates causes selective insulin resistance in diabetes and obesity. 7, 1–16.

LEE JM, KIM Y, HERNÁNDEZ MAS, HAN Y, LIU R. & PARK SWJSR 2019. BRD7 deficiency leads to the development of obesity and hyperglycemia. 9, 1–10.

LEE JM, LIU R. & PARK SW 2021. The regulatory subunits of PI3K, p85α and p85β, differentially affect BRD7-mediated regulation of insulin signaling. J Mol Cell Biol.

LU M, WAN M, LEAVENS KF, CHU Q, MONKS BR, FERNANDEZ S, AHIMA RS, UEKI K, KAHN CR & BIRNBAUM MJ 2012. Insulin regulates liver metabolism in vivo in the absence of hepatic Akt and Foxo1. Nat Med, 18, 388–95. [PubMed: 22344295]

LUO J, FIELD SJ, LEE JY, ENGELMAN JA & CANTLEY LC 2005. The p85 regulatory subunit of phosphoinositide 3-kinase down-regulates IRS-1 signaling via the formation of a sequestration complex. J Cell Biol, 170, 455–64. [PubMed: 16043515]

MICHAEL MD, KULKARNI RN, POSTIC C, PREVIS SF, SHULMAN GI, MAGNUSON MA & KAHN CR 2000. Loss of insulin signaling in hepatocytes leads to severe insulin resistance and progressive hepatic dysfunction. Mol Cell, 6, 87–97. [PubMed: 10949030]

PARK SW, HERREMA H, SALAZAR M, CAKIR I, CABI S, BASIBUYUK SAHIN F, CHIU YH, CANTLEY LC & OZCAN U. 2014. BRD7 regulates XBP1s' activity and glucose homeostasis through its interaction with the regulatory subunits of PI3K. Cell Metab, 20, 73–84. [PubMed: 24836559]

PARK SW & LEE JMJIJOMS 2020. Emerging Roles of BRD7 in Pathophysiology. 21, 7127.

PARK SW, ZHOU Y, LEE J, LU A, SUN C, CHUNG J, UEKI K. & OZCAN U. 2010. The regulatory subunits of PI3K, p85α and p85β, interact with XBP-1 and increase its nuclear translocation. Nat Med, 16, 429–437. [PubMed: 20348926]

RUI L. 2014. Energy metabolism in the liver. Compr Physiol, 4, 177–97. [PubMed: 24692138]

SANCHEZ R. & ZHOU MM 2009. The role of human bromodomains in chromatin biology and gene transcription. Curr Opin Drug Discov Devel, 12, 659–65.

TAO R, WANG C, STÖHR O, QIU W, HU Y, MIAO J, DONG XC, LENG S, STEFATER M. & STYLOPOULOS N. 2018. Inactivating hepatic follistatin alleviates hyperglycemia. Nat Med, 24, 1058–1069. [PubMed: 29867232]

TITCHENELL PM, CHU Q, MONKS BR & BIRNBAUM MJ 2015. Hepatic insulin signalling is dispensable for suppression of glucose output by insulin in vivo. Nat Commun, 6, 1–9.

UEKI K, YBALLE CM, BRACHMANN SM, VICENT D, WATT JM, KAHN CR & CANTLEY LC 2002. Increased insulin sensitivity in mice lacking p85β subunit of phosphoinositide 3-kinase. PNAS, 99, 419–424. [PubMed: 11752399]

WHITE MF & KAHN CRJMM 2021. Insulin action at a molecular level–100 years of progress. 52, 101304.

ZHENG Y, LEY SH & HU FB 2018. Global aetiology and epidemiology of type 2 diabetes mellitus and its complications. Nat Rev Endocrinol, 14, 88–98. [PubMed: 29219149]

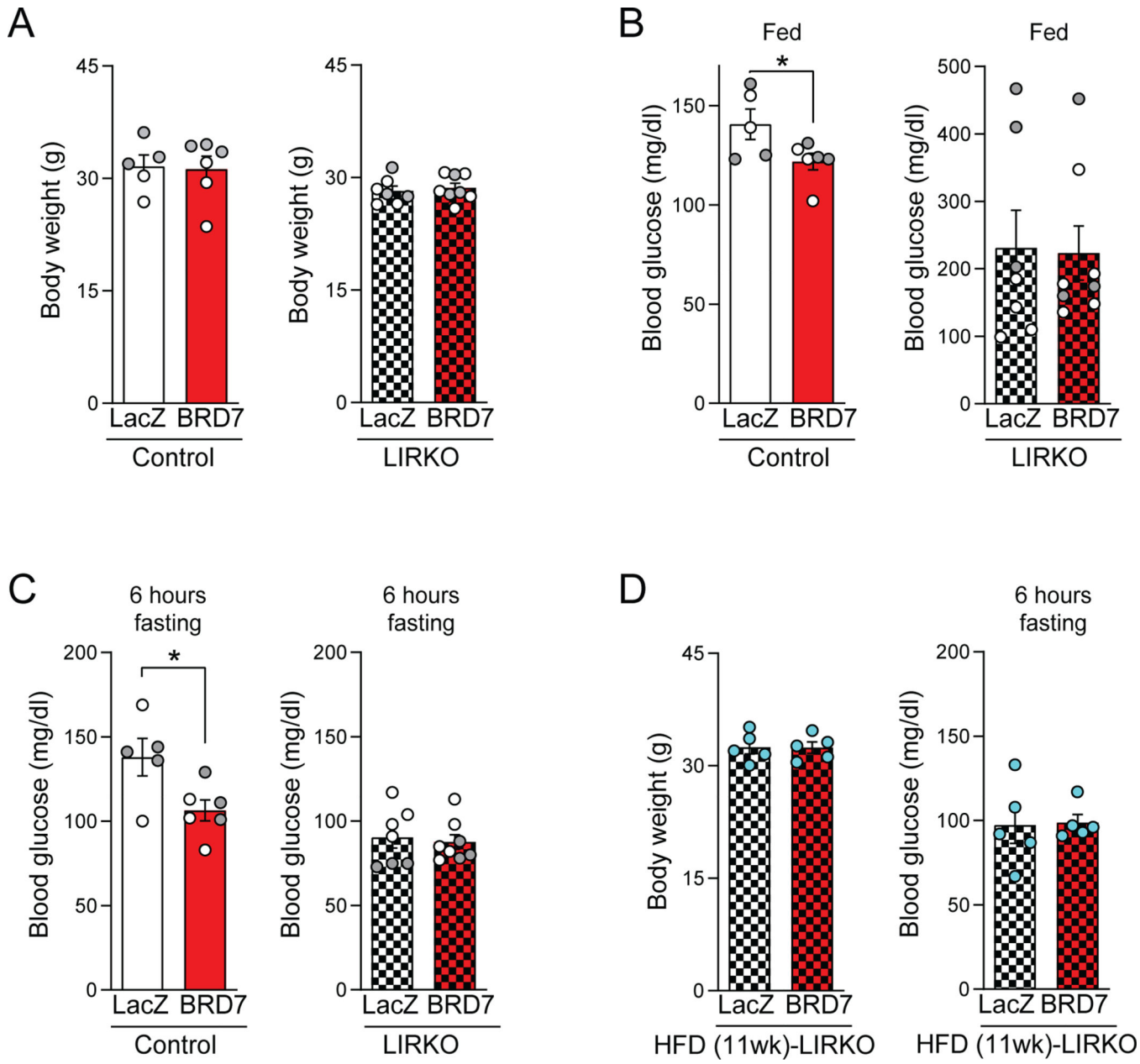

Figure 1. Body weights and blood glucose levels are not altered by the upregulation of BRD7 in HFD-fed LIRKO mice.

(**A-C**) Wild-type (WT, n=5–6) and LIRKO (n=7–8) mice were subjected to a HFD for 8 weeks, followed by injection with Ad-BRD7 or Ad-LacZ through the tail vein. The different colored dots represent independent cohorts. (**A**) Body weights of control (left) and LIRKO (right) mice on day 8 post-injection. (**B**) Fed blood glucose levels of control (left) and LIRKO (right) mice on day 3 post-injection. (**C**) 6-hour fasted blood glucose levels of control (left) and LIRKO (right) mice on day 6–8 post-injection. (**D**) LIRKO mice were fed on a HFD for 11 weeks and injected with Ad-BRD7 or Ad-LacZ through the tail vein (n=5 per group). Body weights (left) and blood glucose levels (right) after 6 hours of fasting on

day 8 post-injection. Students' t-test was used to analyze body weights, fed and 6 hours fasting blood glucose levels. Error bars represent SEM. *$p < 0.05$.

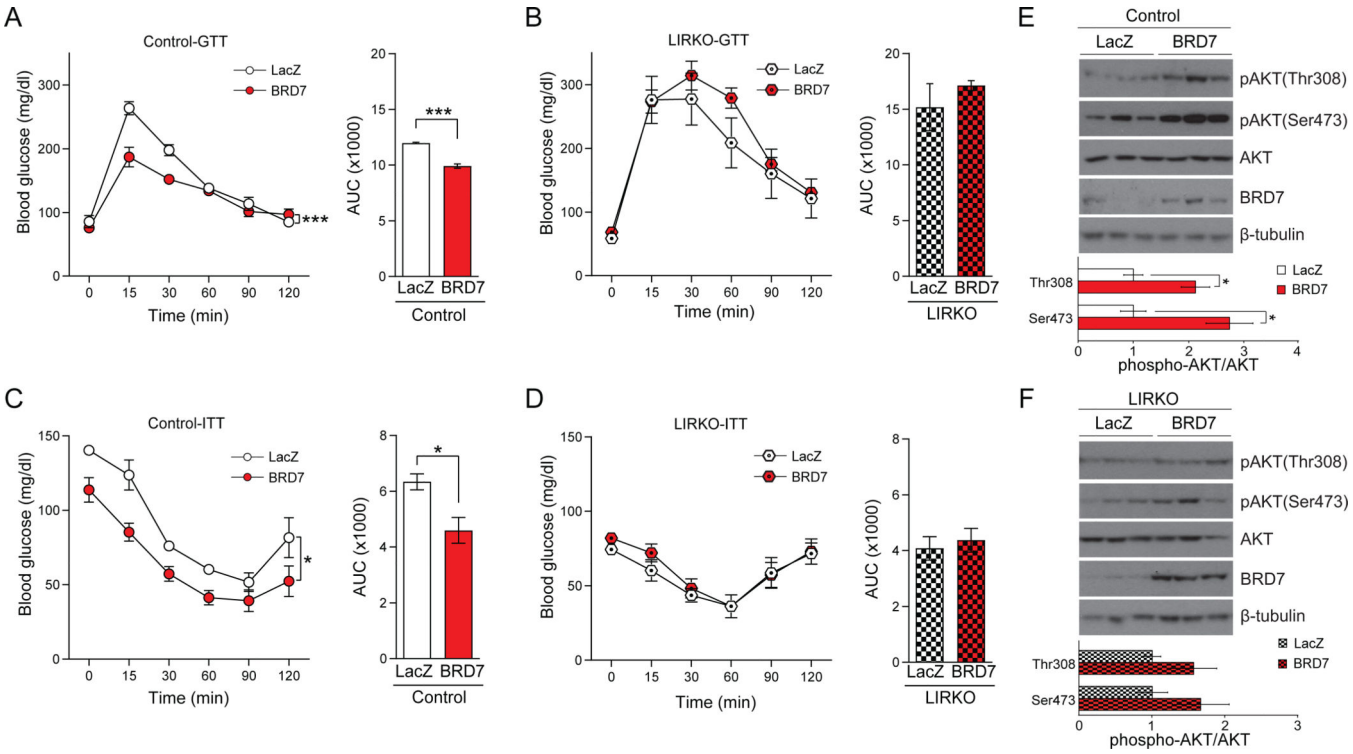

Figure 2. The insulin receptor is required for BRD7 to affect glucose homeostasis.

(**A-F**) WT and LIRKO mice fed on a HFD for 8 weeks were injected with Ad-BRD7 or Ad-LacZ through the tail vein. (**A**) GTT (1.5 g/kg) performed on WT mice on day 8 post-injection and calculation of area under the curve (AUC). (**B**) GTT (1.2 g/kg) performed on LIRKO mice on day 8 post-injection and AUC. (**C**) ITT (1.0 IU/kg) conducted on WT mice on day 6 post-injection and AUC. (**D**) ITT (2.0 IU/kg) on LIRKO mice on day 6 post-injection and AUC. (**E-F**) Immunoblots of total liver lysates for indicated antibodies at the 6-hour fasted state in WT (**E**) and LIRKO (**F**) mice, with quantifications. pAKT(Thr308) and pAKT(Ser473) were normalized to total AKT. Students' t-test was used to analyze AUC and quantification of immunoblots. Two-way repeated measure mixed ANOVA was used to analyze GTT and ITT. Error bars represent SEM. *p < 0.05, ***p < 0.001.

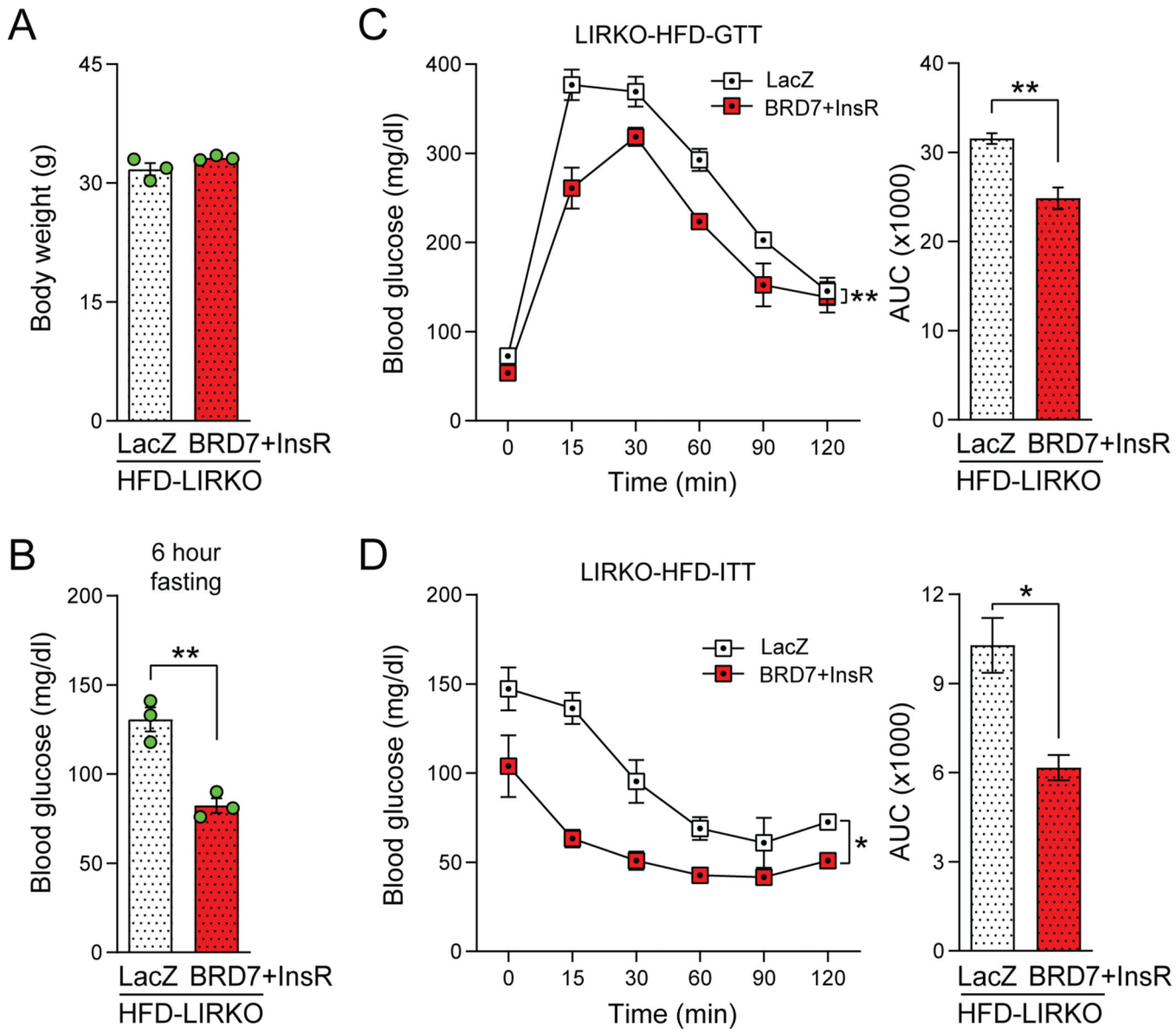

Figure 3. Restoration of insulin receptors and upregulation of BRD7 in the liver restores glucose homeostasis in HFD-challenged LIRKO mice.

LIRKO mice fed on a HFD for 8 weeks were injected with Ad-LacZ as a control or Ad-InsR and Ad-BRD7 through the tail vein (n=3 per group). (**A**) Body weights were measured on day 9 post-injection. (**B**) Blood glucose levels after 6 hours of fasting on days 3 post-injection. (**C**) GTT (1.2 g/kg) performed on LIRKO mice on day 4 post-injection (left). Calculation of AUC (right). (**D**) ITT (2.0 IU/kg) performed on day 6 post-injection (left) and AUC (right). Students' t-test was used to analyze body weight, blood glucose, and AUC. Two-way repeated measure mixed ANOVA was used to analyze GTT and ITT. Error bars represent SEM. *$p < 0.05$, **$p < 0.01$.

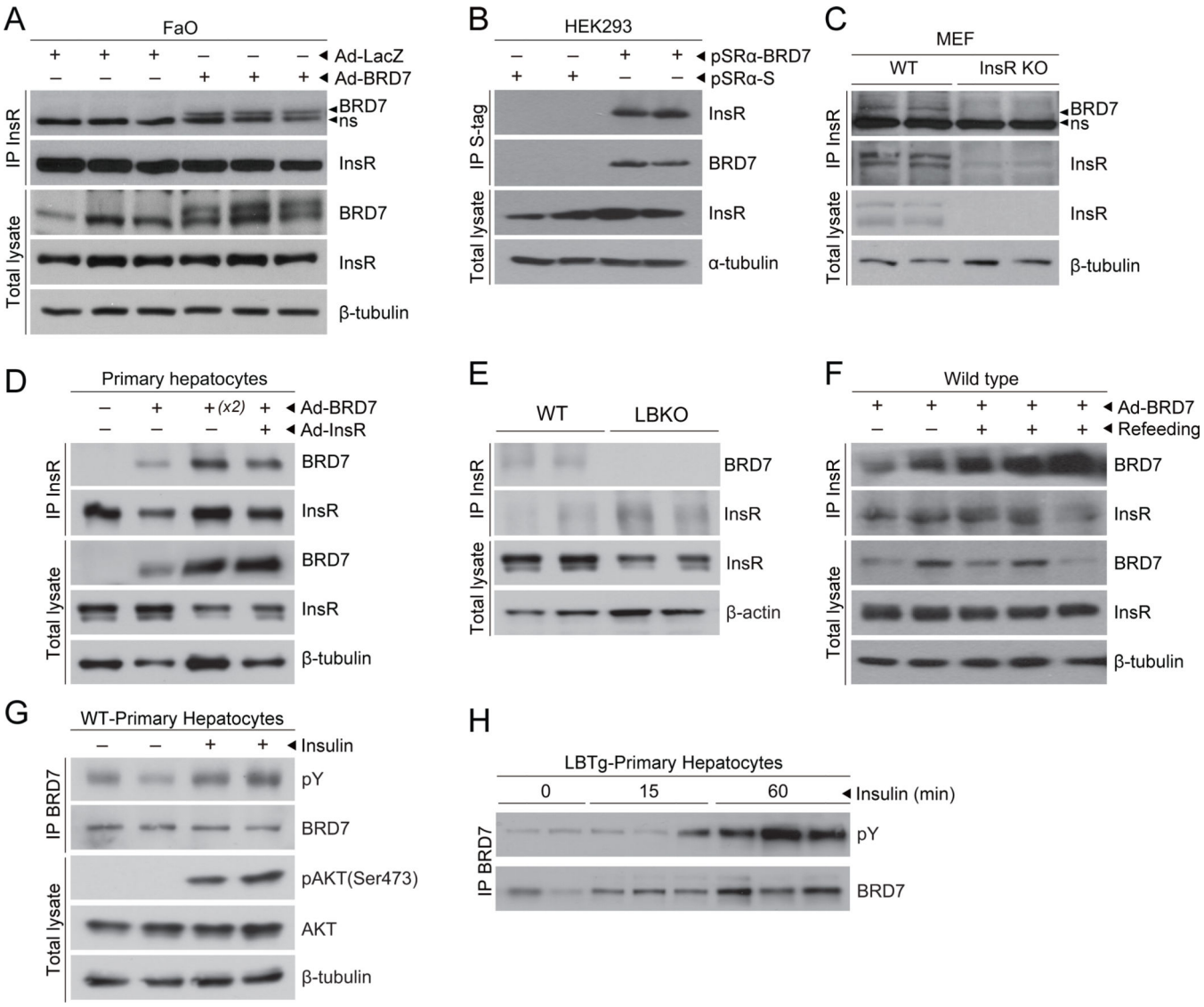

Figure 4. BRD7 interacts with the insulin receptor.

(**A**) FaO cells were infected with Ad-BRD7 or Ad-LacZ. Total cell lysates were immunoprecipitated using an InsR-specific antibody and immunoblotted with the indicated antibodies. Non-specific bands are labelled ns. (**B**) HEK293 cells were transfected with a plasmid expressing S-tagged BRD7 (pSRα-HA-S-BRD7) or its corresponding control plasmid (pSRα-S). Total cell lysates were precipitated with S-protein agarose and immunoblotted for the indicated antibodies. (**C**) Cell lysates from control or InsR KO MEF cells were immunoprecipitated using an InsR-specific antibody and immunoblotted with the indicated antibodies. (**D**) Primary hepatocytes were isolated from C57Bl/6J mice and infected with Ad-BRD7 and Ad-InsR as indicated. Immunoprecipitation was performed using an InsR-specific antibody on total cell lysates, followed by immunoblotting with the specified antibodies. The notion of x2 indicates that the amount of cell lysates used in this sample was doubled compared to the standard volume. (**E**) Liver lysates from wild-type and liver-specific BRD7 knockout (LBKO) mice were immunoprecipitated using an InsR-

specific antibody and immunoblotted with the indicated antibodies. (**F**) C57Bl/6J mice were injected with Ad-BRD7. On day 6 post-injection, mice were fasted for 24 hours and refed *ad libitum* for 1 hour. Total liver lysates were immunoprecipitated using an InsR-specific antibody and immunoblotted with the indicated antibodies. (**G**) Primary hepatocytes isolated from a C57Bl/6J mouse were treated with insulin (100 nM) for 15 minutes and lysates were immunoprecipitated using a BRD7-specific antibody and immunoblotted with the indicated antibodies. pY indicates phospho-tyrosine. (**H**) Primary hepatocytes were isolated from a liver-specific BRD7 transgenic mouse (LBTg) and stimulated with insulin (100 nM) for 15 or 60 minutes. The total lysates were immunoprecipitated with a BRD7-specific antibody and immunoblotted for pY.

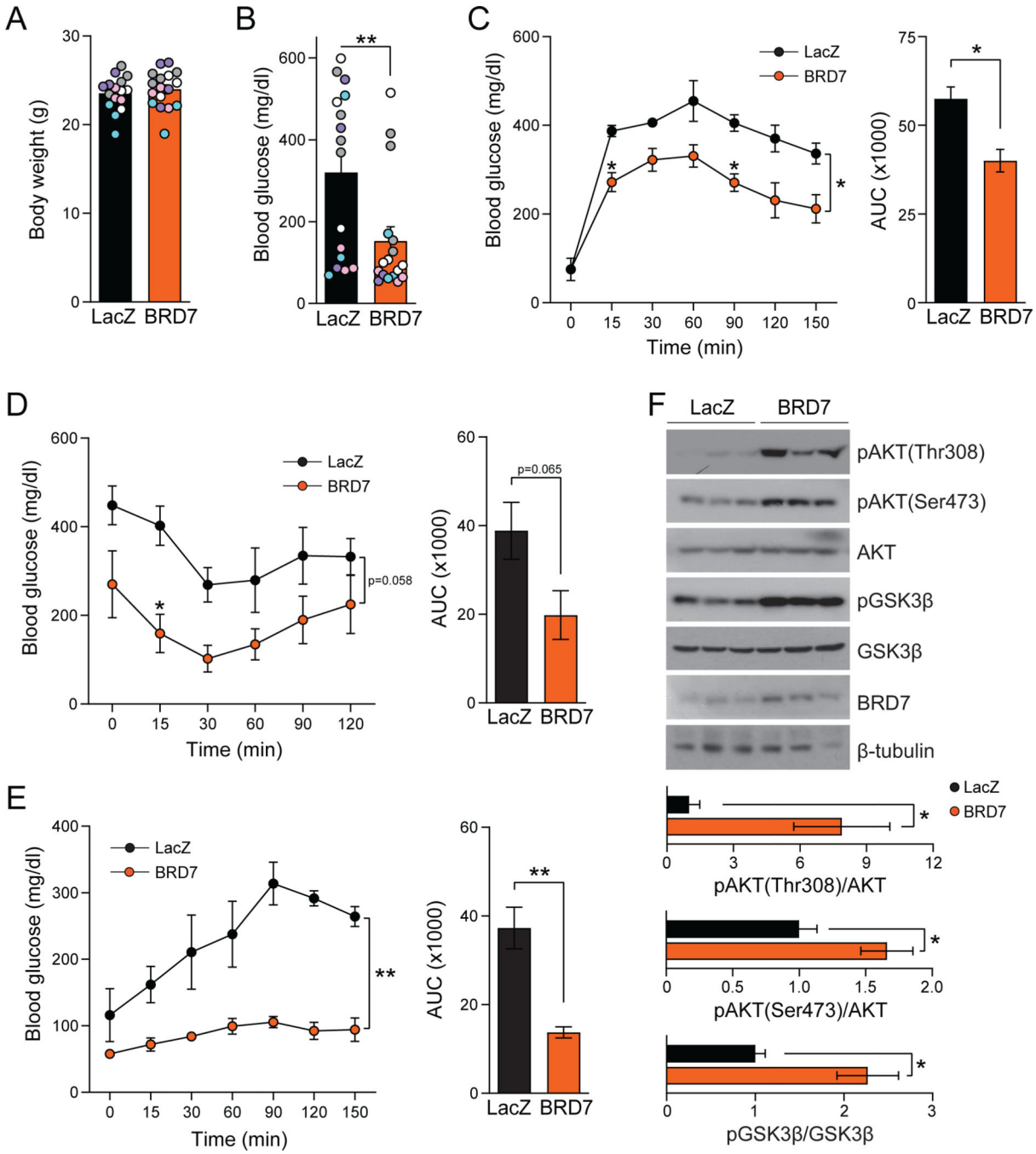

Figure 5. BRD7 improves glucose homeostasis in the absence of IRS1/2.

IRS DKO mice were placed on a HFD for 8–11 weeks and injected with Ad-BRD7 (n=17) or Ad-LacZ (n=16) through the tail vein. The different colored dots represent data from five independent cohorts. (**A**) Body weights on day 8–11 post-injection. (**B**) Blood glucose levels after 6 hours of fasting on days 8–10 post-injection. (**C**) GTT (1.0 g/kg) on day 5 post-injection and calculation of AUC. (**D**) ITT (2.0 IU/kg) on day 8 post-injection and AUC. (**E**) Pyruvate tolerance test (PTT, 2.0 g/kg) on day 9 post-injection and AUC. (**F**) Liver tissues were collected on day 9 post-injection after 6 hours of fasting and immunoblotted for the

indicated antibodies. Quantifications of the immunoblots were performed by normalizing pAKT(Thr308) and pAKT(Ser473) to total AKT, and pGSKβ(Ser9) to total GSKβ. Students' t-test was used to analyze body weights, blood glucose, AUC and quantification of the immunoblots. Two-way repeated measure mixed ANOVA was used to analyze GTT, ITT, and PTT. Error bars represent SEM. *$p < 0.05$, **$p < 0.01$.

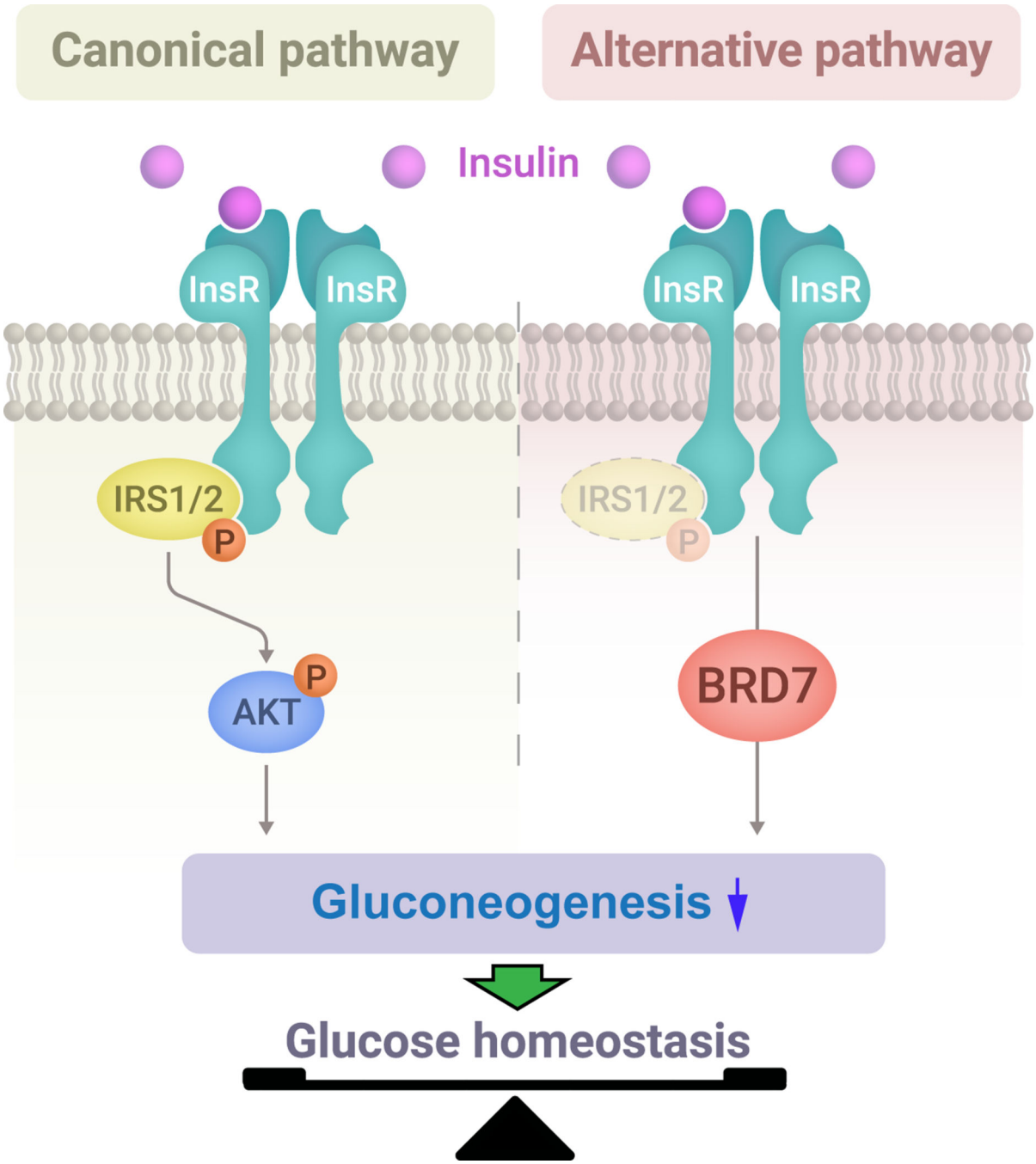

Figure 6. Schematic diagram.

On the left, the canonical insulin receptor signaling pathway is depicted, where insulin binding to the insulin receptor leads to the recruitment and activation of IRS proteins and downstream effector proteins, including AKT, to regulate glucose homeostasis. The right panel represents the proposed alternative insulin signaling pathway that operates independently of IRS1/2, providing an additional mechanism for regulating glucose metabolism.